Please cite this article in press as: Schleich et al., Stoichiometry of the CD95 Death-Inducing Signaling Complex: Experimental and Modeling Evidence for a Death Effector Domain Chain Model, Molecular Cell (2012), doi:10.1016/j.molcel.2012.05.006

Molecular Cell
Article

Stoichiometry of the CD95 Death-Inducing Signaling Complex: Experimental and Modeling Evidence for a Death Effector Domain Chain Model

Kolja Schleich,[1,4,7] Uwe Warnken,[2,7] Nicolai Fricker,[1,4] Selcen Öztürk,[1] Petra Richter,[1,4] Kerstin Kammerer,[2] Martina Schnölzer,[2] Peter H. Krammer,[1] and Inna N. Lavrik[1,3,4,5,6,*]
[1]Division of Immunogenetics
[2]Functional Proteome Analysis
[3]Division of Theoretical Bioinformatics
German Cancer Research Center (DKFZ), 69120 Heidelberg, Germany
[4]Bioquant, 69120 Heidelberg, Germany
[5]Faculty of Fundamental Medicine, ML Lomonosov State University, 119192 Moscow, Russia
[6]Department of Translational Inflammation Research, Institute of Experimental Internal Medicine, Otto von Guericke University, 39120 Magdeburg, Germany
[7]These authors contributed equally to this work
*Correspondence: i.lavrik@dkfz.de or inna.lavrik@med.ovgu.de
DOI 10.1016/j.molcel.2012.05.006

SUMMARY

The CD95 (Fas/APO-1) death-inducing signaling complex (DISC) is essential for the initiation of CD95-mediated apoptotic and nonapoptotic responses. The CD95 DISC comprises CD95, FADD, procaspase-8, procaspase-10, and c-FLIP proteins. Procaspase-8 and procaspase-10 are activated at the DISC, leading to the formation of active caspases and apoptosis initiation. In this study we analyzed the stoichiometry of the CD95 DISC. Using quantitative western blots, mass spectrometry, and mathematical modeling, we reveal that the amount of DED proteins procaspase-8/procaspase-10 and c-FLIP at the DISC exceeds that of FADD by several-fold. Furthermore, our findings imply that procaspase-8, procaspase-10, and c-FLIP could form DED chains at the DISC, enabling the formation of dimers and efficient activation of caspase-8. Taken together, our findings provide an enhanced understanding of caspase-8 activation and initiation of apoptosis at the DISC.

INTRODUCTION

CD95 (APO-1/Fas) is a member of the death receptor (DR) family, a subfamily of the tumor necrosis factor receptor (TNF-R) superfamily (Krammer, 2000; Strasser et al., 2009). Stimulation of CD95 with its natural ligand CD95L or with agonistic anti-CD95 antibodies, such as anti-APO-1, induces apoptosis in sensitive cells (Lavrik et al., 2005; Trauth et al., 1989). Triggering of CD95 has also been reported to induce nonapoptotic pathways, such as the NF-κB, Akt, and ERK pathway (Peter et al., 2007). The binding of CD95L to CD95 leads to the formation of the death-inducing signaling complex (DISC). The DISC comprises oligomerized CD95, the adaptor protein FADD, procaspase-8, procaspase-10, and cellular FLICE inhibitory proteins (c-FLIPs) (Figure 1A) (Krammer et al., 2007; Scaffidi et al., 1997; Scott et al., 2009; Sprick et al., 2002). The interactions between the molecules at the DISC are based on homotypic contacts. The death domain (DD) of CD95 interacts with the DD of FADD, while the death effector domain (DED) of FADD interacts with the N-terminal DEDs of procaspase-8, procaspase-10, and the c-FLIP isoforms.

The DISC is a central mediator of the CD95 signaling pathway. Efficient DISC formation promotes procaspase-8 activation and regulates both apoptotic and nonapoptotic signaling. Yet the stoichiometry of the DISC is still unresolved, as the DISC comprises several procaspase-8, procaspase-10, and c-FLIP isoforms (procaspase-8a/b, procaspase-10a/c/d, and c-FLIP$_{L/S/R}$) and their cleavage products (Golks et al., 2005, 2006a, 2006b; Hoffmann et al., 2009; Hughes et al., 2009; Muzio et al., 1996; Scaffidi et al., 1997, 1999; Sprick et al., 2002). The conventional understanding of CD95 DISC stoichiometry is that the trimerized receptor forms the core of the DISC structure. Each CD95 binds one FADD, which in turn binds one DED protein, e.g., procaspase-8, procaspase-10, or c-FLIP (Figure 1A) (Krammer et al., 2007). Considering that there are three DED proteins at the DISC, i.e., procaspase-8, procaspase-10, and c-FLIP, and each of the DED proteins comprises several isoforms, the seemingly simple ''one-to-one'' model does not in fact provide a clear explanation to a number of questions. One of the most important questions is how homodimers and heterodimers of procaspase-8/procaspase-10/c-FLIP could be formed in the context of the DISC in order to enable efficient caspase activation at the DISC (Fuentes-Prior and Salvesen, 2004).

One well-established approach to address the stoichiometry of protein complexes is quantitative mass spectrometry (MS). This is currently the most sensitive method, which can provide absolute amounts of proteins (Aebersold and Mann, 2003).

Please cite this article in press as: Schleich et al., Stoichiometry of the CD95 Death-Inducing Signaling Complex: Experimental and Modeling Evidence for a Death Effector Domain Chain Model, Molecular Cell (2012), doi:10.1016/j.molcel.2012.05.006

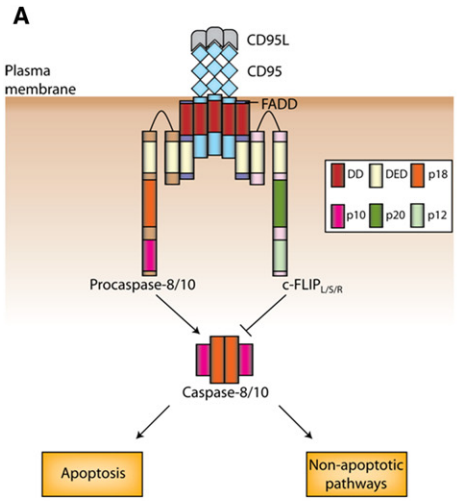

B

Protein	Number of molecules / cell SKW6.4 cells	HeLa-CD95 cells
FADD	100,000	130,000
Procaspase-8a/b	106,000	250,000
c-FLIP$_L$	670	230
c-FLIP$_{S/R}$	1,000	530

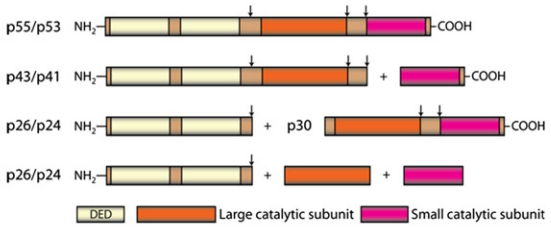

C

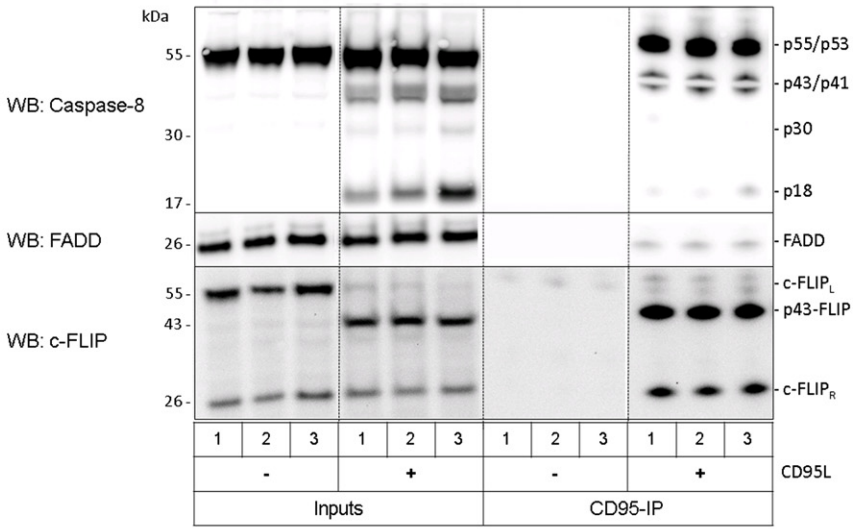

D

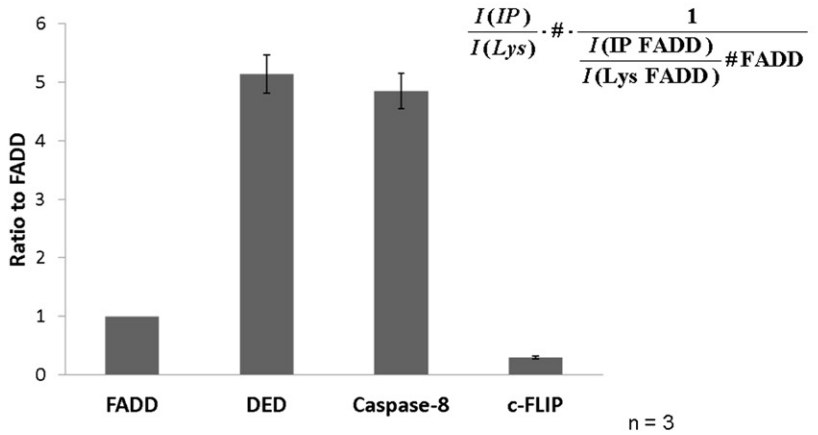

Another way to approach the complexity of the DISC stoichiometry is to construct mathematical models that are verified by experimental data (Albeck et al., 2008; Bentele et al., 2004; Fricker et al., 2010; Neumann et al., 2010; Rehm et al., 2006). There are several mathematical formalisms that have been used for modeling apoptotic networks: ordinary differential equations (ODEs) (Albeck et al., 2008; Bentele et al., 2004; Fricker et al., 2010; Fussenegger et al., 2000; Neumann et al., 2010; Rehm et al., 2006), Boolean modeling (Schlatter et al., 2009), Petri nets (Heiner et al., 2004), and cellular automata (Chen et al., 2007). So far, most of these models have addressed the kinetics of caspase-8 activation in DR-induced apoptosis and the ratio between procaspase-8 and c-FLIP isoforms at the DISC (Lavrik, 2010). However, with the exception of the analysis of the procaspase-8/c-FLIP ratio, further insight into the DISC stoichiometry has been missing.

To study the DISC stoichiometry, we combined quantitative western blot with MS analysis and mathematical modeling. This powerful combination of quantitative approaches revealed fascinating insight into the stoichiometry of the DISC and activation of procaspase-8 within this complex. We could show that the amount of procaspase-8 at the DISC is much higher than that of FADD, while c-FLIP is present at low abundance compared to procaspase-8. Our findings suggest that procaspase-8 and c-FLIP form DED platforms at the DISC. In these platforms, procaspase-8 forms homodimers and heterodimers with c-FLIP, leading to caspase activation.

RESULTS

Quantitative Western Blot Analysis Reveals Fewer FADD Molecules Than Procaspase-8 Molecules at the DISC

To determine the stoichiometry of the CD95 DISC, we utilized B lymphoblastoid SKW6.4 cells. SKW6.4 cells are type I cells forming high quantities of the CD95 DISC and are highly sensitive toward CD95-induced apoptosis (Aldridge et al., 2011; Scaffidi et al., 1998). SKW6.4 cells were already used by us for our first systems biology model of CD95-induced apoptosis and, therefore, have been demonstrated to be an excellent model cell line for the quantitative analysis of CD95-induced apoptosis (Bentele et al., 2004).

First, we determined absolute numbers of DISC proteins in SKW6.4 cells by comparing them to the already measured values in HeLa-CD95 cells using quantitative western blot (see Figure S1 available online; Figure 1B [Fricker et al., 2010]). On the basis of the absolute numbers of DISC proteins in SKW6.4 cells, we could estimate their amounts at the DISC.

To obtain CD95 DISCs, SKW6.4 cells were stimulated with 1 μg/ml CD95L, and CD95 DISCs were immunoprecipitated using agonistic anti-APO-1 antibodies (Trauth et al., 1989). Importantly, it was known from our previous studies (Lavrik et al., 2008) that under these immunoprecipitation (IP) conditions, namely using 10 μg of anti-APO-1 and 10^8 SKW6.4 cells, it is possible to pull down almost 100% of CD95 DISCs. In this study, we used 5×10^7 cells to immunoprecipitate CD95 DISCs even more efficiently. Together with cellular lysates, IPs of CD95 DISCs from a defined number of SKW6.4 cells were loaded on the same SDS-PAGE and analyzed by western blot (Figure 1C). As expected, DISC-IPs contained CD95, FADD, procaspase-8a/b, and two isoforms of c-FLIP, c-$FLIP_L$, and c-$FLIP_R$ that were reported to be present in SKW6.4 cells. Procaspase-8a/b (p55/p53) processing at the DISC involves cleavage at several Asp (D) residues between the prodomain and the small and large catalytic subunits. This results in formation of the N-terminal cleavage products p43/p41, the prodomains p26/p24, and the C-terminal cleavage products p30, p18, and p10 (Figure 1B). Cleavage products of procaspase-8 were detected in CD95 DISC-IPs, indicating efficient activation of procaspase-8 at the DISC (Figures 1B and 1C).

To define the ratio between the amount of DISC proteins recruited to the DISC and the amount of the same protein in the total cellular lysates, we used quantitative western blot. The percentage of recruitment to the DISC for procaspase-8, FADD, or c-$FLIP_{L/R}$ was multiplied, with the absolute number of the corresponding proteins in SKW6.4 cells shown in Figure 1B. Remarkably, we found that there is approximately five times more procaspase-8 than FADD at the DISC (Figure 1D). The amount of c-FLIP isoforms at the DISC was much lower than the amount of procaspase-8 (Figure 1D), which is in accordance with the low number of c-FLIP in total cellular lysates (Figure 1B). Despite the low numbers, c-FLIP proteins are present at the DISC, likely due to their reported higher affinity to the DISC compared to procaspase-8 (Lavrik et al., 2007).

These data provided a hint that FADD is present in lower quantities than DED proteins at the DISC, in particular procaspase-8.

Quantitative Mass Spectrometry Confirmed the Higher Abundance of Procaspase-8 at the DISC

To further explore the DISC stoichiometry, we used an independent quantitative approach, namely, quantitative MS (Aebersold and Mann, 2003). Absolute quantitative protein MS, termed AQUA, is achieved by parallel analysis of proteotypic analyte and isotopically labeled synthetic peptide standards (Gerber et al., 2003). To get an independent assessment, quantitative

Figure 1. The Analysis of DISC Stoichiometry by Quantitative Western Blot Reveals More Procaspase-8 Than FADD at the DISC

(A) Former DISC model (Krammer et al., 2007). The ratio between procaspase-8 and FADD is one to one.

(B) The number of procaspase-8, FADD, c-$FLIP_L$, and c-$FLIP_R$ molecules (top) in SKW6.4 cells estimated by western blot using HeLa-CD95 cells as reference. Procaspase-8 processing at the DISC (bottom).

(C) 5×10^7 SKW6.4 cells were stimulated with 1 μg/ml CD95L or left untreated. Total cellular lysates (Input) and DISC-IPs were analyzed by western blot. The results of three independent experiments are shown.

(D) Shown is the ratio between DISC components calculated by comparing the intensities of the western blot signals for FADD, c-FLIP, procaspase-8 or DED-proteins (the sum of procaspase-8 and c-FLIP) in the IP to lysates. The number of procaspase-8 molecules comprises the sum of intensities of the western blot signals for procaspase-8a/b, p43/p41, and p18. The number of c-FLIP proteins comprises the sum of intensities of the western blot signals for c-$FLIP_L$ and p43-FLIP. The number of DED proteins comprises the sum of procaspase-8 and c-FLIP proteins. The ratio for each molecule was multiplied by the molecule number in SKW6.4 cells. The obtained molecule numbers at the DISC were normalized to FADD. The mean ± SD of three independent experiments is shown.

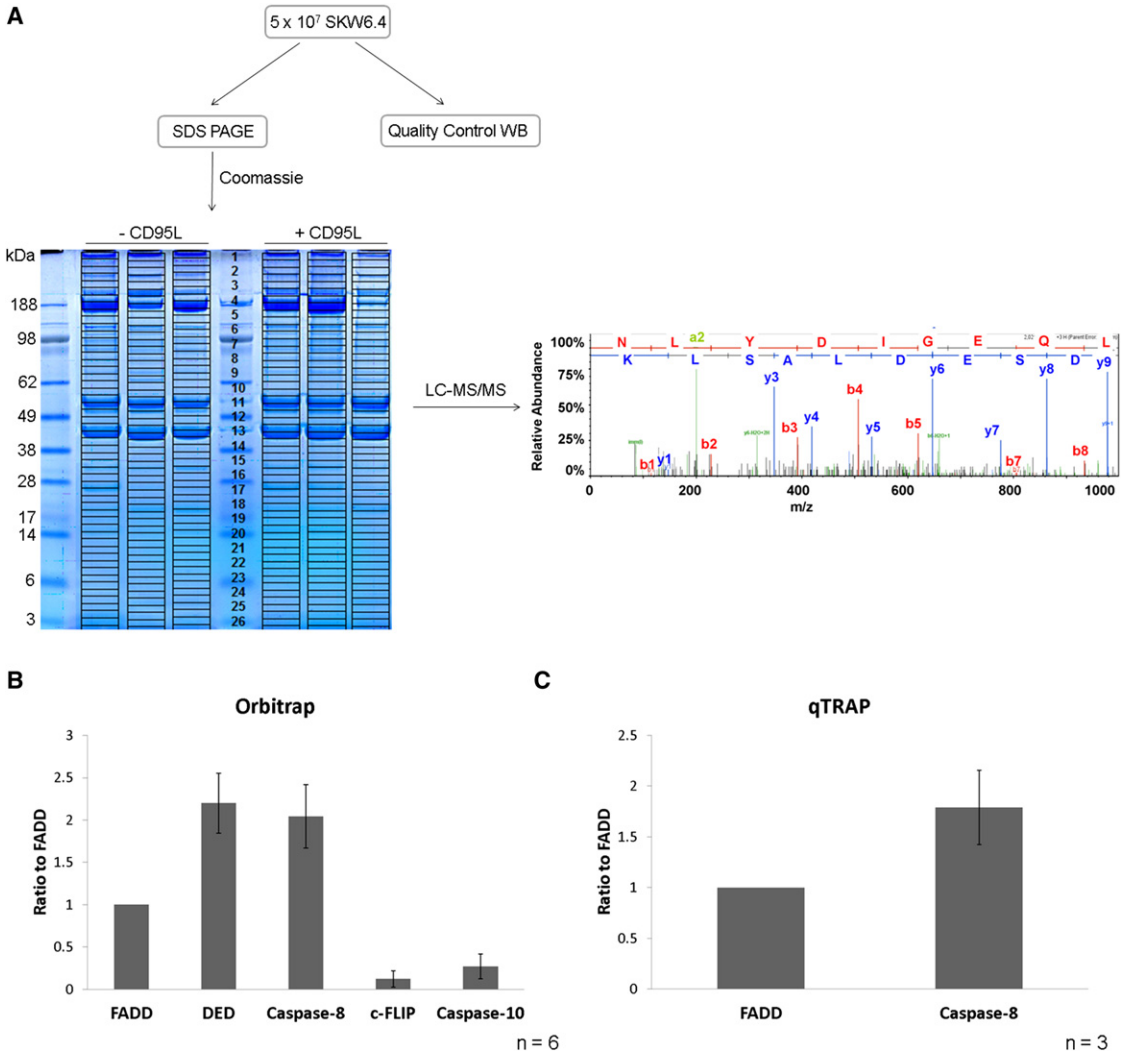

Figure 2. DISC Stoichiometry Using Mass Spectrometry

(A) Workflow of the mass spectrometry experiments. 5 × 10^7 of SKW6.4 cells were stimulated with 1 μg/ml CD95L or left untreated. CD95-IPs were analyzed using 1D SDS PAGE and Coomassie staining. Gel slices corresponding to a mass range of 20–60 kDa were digested and subjected to mass spectrometry. FADD was detected in gel slices corresponding to 25–28 kDa. Procaspase-8a/b, c-$FLIP_{L/R}$, and their cleavage products were detected in gel slices corresponding to a mass range of 38–60 kDa and 20–35 kDa, respectively.

(B and C). Ratios of procaspase-8/procaspase-10 and c-FLIP, and the sum of DED proteins to FADD at the DISC obtained for Orbitrap (B) and QTRAP (C). The mean ± SD of six and three independent experiments, respectively, is shown.

data for the CD95 DISC were obtained from two different mass spectrometers: an LTQ-Orbitrap (a tandem ion trap mass spectrometer) and a QTRAP 5500 operated in the triple-quadrupole mode (Lange et al., 2008; Olsen et al., 2005). Absolute quantification of CD95 DISC proteins using the Orbitrap mass spectrometer was performed with a set of AQUA-peptide standards corresponding to FADD, procaspase-8, procaspase-10, and c-FLIP (Table S1). QTRAP measurements were carried out with a set of four AQUA-peptide standards corresponding to procaspase-8 and FADD (Table S2).

For MS experiments, CD95-IPs from 5 × 10^7 SKW6.4 cells were carried out under conditions similar to those developed for western blot quantifications, i.e., stimulation with 1 μg/ml CD95L (Figure 1). CD95-IPs were separated on 1D-SDS gels to reduce sample complexity and thereby increase sensitivity and selectivity of the MS analysis (Figure 2A). A similar procedure for absolute MS quantification of proteins in a polyacrylamide matrix using AQUA peptides has been recently described (Langenfeld et al., 2009). The specificity of DISC-IPs was controlled by western blot (data not shown). As negative controls, CD95-IPs were performed from unstimulated cells, which were analyzed by both western blot and MS analysis. In the negative control, DISC proteins were detected neither by western blot nor by MS. CD95 DISC proteins are not highly abundant in the CD95-IPs. More than 1,000 proteins were detected by MS in these DISC-IPs (data not shown), though western blot analysis

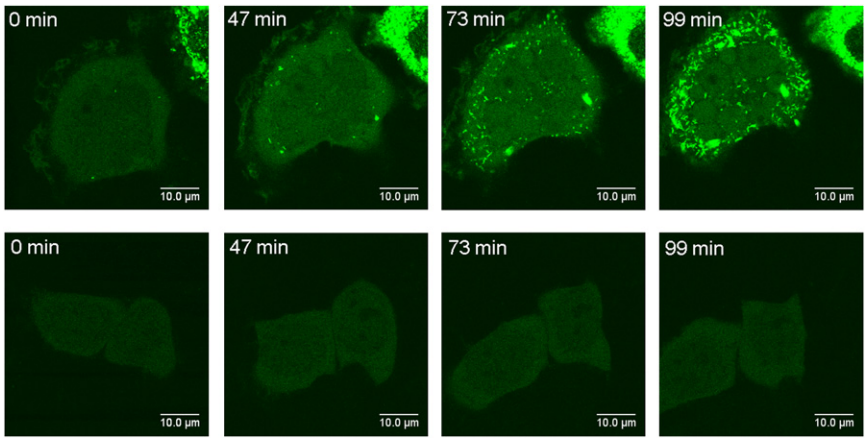

Figure 3. Procaspase-8 Prodomain Forms "Spot-like Aggregates" upon CD95L Stimulation

HeLa-CD95 cells were transfected with procaspase-8 prodomain-GFP constructs, stimulated with 1 µg/ml CD95L (top) or left unstimulated (bottom), and imaged over time. zVAD-fmk was added at a concentration of 50 µM to block apoptosis.

shows significant recruitment of procaspase-8, FADD, and c-FLIP to the DISC. Among DISC-associated proteins, we could not detect DAXX, FAP-1, FLASH, FAF-1, or Dap3, which were previously reported to be present at the DISC, possibly due to their low abundance at the CD95 DISC (Peter and Krammer, 2003).

Orbitrap measurements demonstrated that there were two to three DED proteins (the sum of procaspase-8, procaspase-10, and c-FLIP) per FADD (Figure 2B, Table S3). Interestingly, the amount of both c-FLIP and procaspase-10 at the DISC was approximately ten times lower compared to procaspase-8 (Figure 2B). Low numbers of c-FLIP proteins are in accordance with western blot data (Figure 1B) and as pointed out above are likely due to their low numbers in the cells. The low abundance of procaspase-10 at the DISC could be an explanation for its earlier reported inability to initiate apoptosis in the absence of caspase-8 (Sprick et al., 2002). Therefore, we concluded that procaspase-8 is a major component of the DISC present in higher quantities compared to the other DED proteins. To confirm these results, we repeated the analysis using a QTRAP mass spectrometer (Figure 2C, Table S4). Procaspase-8 was also found at the DISC in higher amounts compared to FADD, with procaspase-8 to FADD ratios similar to those in the Orbitrap analysis (Figure 2C, Table S4). The lower abundance of FADD at the DISC corresponded well with the Orbitrap data.

Collectively, quantitative MS of the DISC confirmed the quantitative western blot data showing that the ratio between procaspase-8 and FADD is not one to one. Though MS and western blot provided different numbers of procaspase-8 excess over FADD, both approaches clearly pointed out the challenging feature of the DISC stoichiometry, namely that procaspase-8 outnumbers FADD at the CD95 DISC. Therefore, we concluded that we have to reconsider the former view on CD95 DISC organization.

Single-Cell Analysis Supports Chain Formation of Procaspase-8 at the DISC

The formation of chains is fundamental in biology and a driving factor for many biological processes. We questioned whether procaspase-8 can form chains at the DISC. Indeed, it was reported that formation of homodimers of procaspase-8 is a prerequisite for caspase-8 activation (Fuentes-Prior and Salvesen, 2004) and that two procaspase-8 homodimers, e.g., four procaspase-8 molecules, have to be in close proximity to ensure effective caspase-8 activation (Chang et al., 2003). It was also shown that FADD and procaspase-8 DEDs can form filaments upon overexpression (Siegel et al., 1998). In our own experiments, we also observed CD95L stimulation-dependent increased intensity of procaspase-8 or spot-like structures upon a low level of overexpression of procaspase-8-prodomain-GFP (Figure 3, Figure S2A). Spot-like structures of procaspase-8 indicated aggregation of procaspase-8. However, a clear distinction between filaments, a multitude of spots, or 2D networks cannot readily be made from these images. Upon a high level of overexpression of procaspase-8-GFP, prodomain aggregation was detected without CD95 stimulation, as already reported before by Siegel et al. (1998) (Figure S2B). In addition, studies with MC159, a viral FLIP containing two DEDs, suggested that DEDs could interact via a conserved phenylalanine/leucine (FL) motif (Carrington et al., 2006; Li et al., 2006; Yang et al., 2005). Thus, we hypothesize that procaspase-8 molecules could form DED chains at the DISC via interaction of their DEDs.

Mathematical Modeling Supports Chain Formation of Procaspase-8 at the DISC

To reveal the factors controlling DISC-mediated procaspase-8 chain formation with subsequent activation, we used mathematical modeling. To construct the topology of the mathematical model, we undertook the above-mentioned assumption that procaspase-8 forms chains at the DISC and designed a biochemical scheme based on this assumption (Figure 4A). Upon recruitment to the DISC, procaspase-8 binds to FADD, and subsequently procaspase-8 chains are elongated. We suggested that other DED proteins, e.g., c-FLIP$_{L/R}$ and procaspase-10, could be incorporated into the chains. The DED chains could be of variable length and comprise several molecules associated via their DEDs (Figure 4A). Furthermore, based on our previous observations and on literature reports, we assumed that procaspase-8 heterodimers with c-FLIP$_L$ are catalytically active, while dimers of procaspase-8 and c-FLIP$_R$ are inactive (Fricker et al., 2010). Procaspase-8 was assumed to be processed in these chains, resulting in the release of heterotetramers $p10_2$–$p18_2$ (Figure 4A). The prodomains would remain within the DED chain, possibly serving as a platform for the binding of procaspase-8. The latter is in accordance with previous reports that the prodomain of procaspase-8 remains

Please cite this article in press as: Schleich et al., Stoichiometry of the CD95 Death-Inducing Signaling Complex: Experimental and Modeling Evidence for a Death Effector Domain Chain Model, Molecular Cell (2012), doi:10.1016/j.molcel.2012.05.006

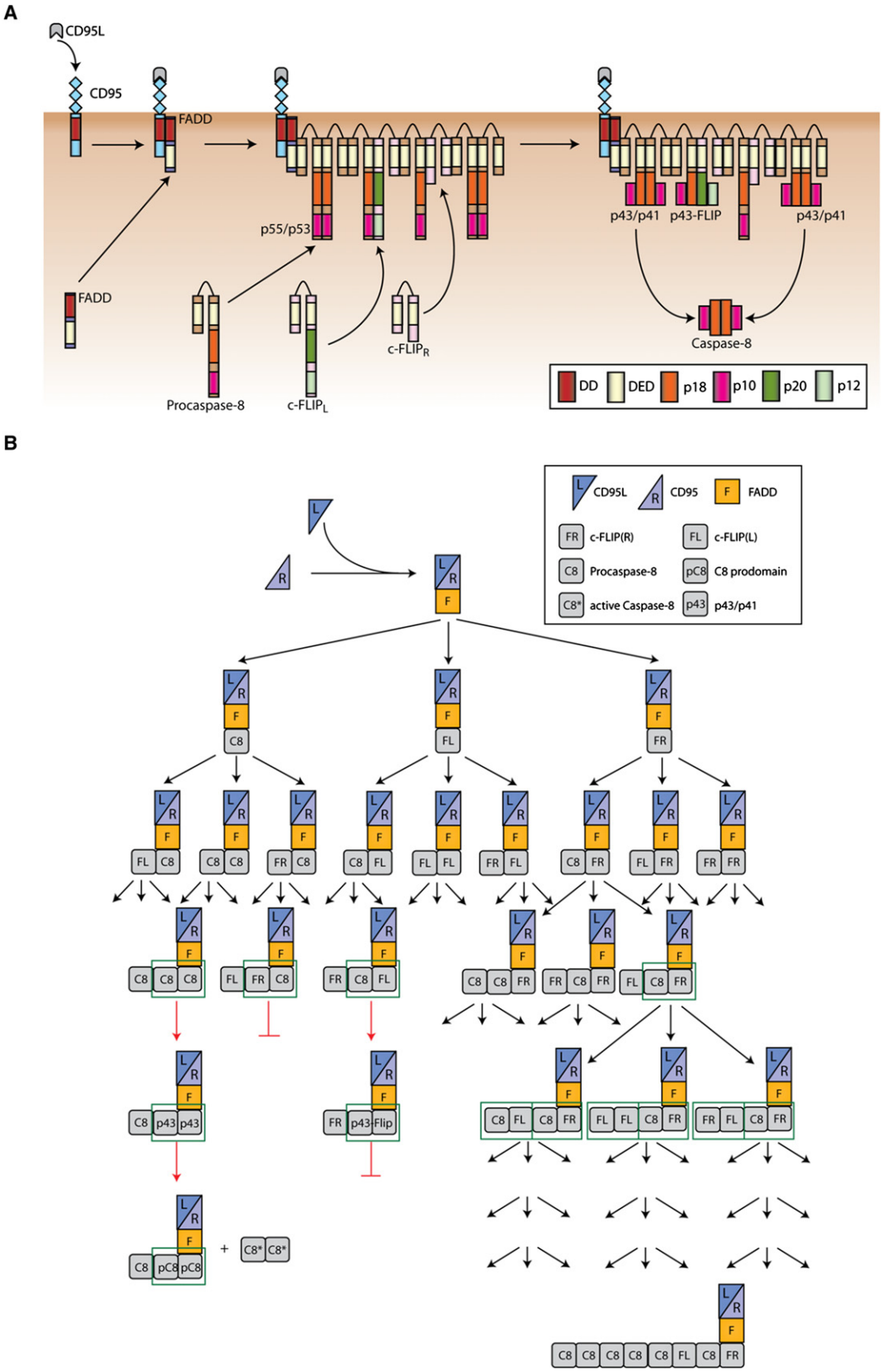

bound to the DISC (Golks et al., 2006b). This biological information (Figure 4A) was translated into a topology of the model of the DISC with chains of procaspase-8 (Figure 4B). The topology of the model comprised the same considerations on the stoichiometry of the CD95 DISC as presented in Figure 4A.

We realized that to perform mathematical modeling we could not use ODEs mostly applied in previous studies for modeling apoptotic networks. The DISC composed of chains of DED proteins of variable length was a system much too complex for ODE modeling (Figure 4B, Supplemental Information). Modeling the DISC system using ODEs would lead to a large number of intermediate products, which exponentially increase with the chain length as demonstrated in Figure 4B. A chain length of only five molecules would give rise to 363 intermediates in an ODE model. Furthermore, it was assumed that the prodomain would remain at the DISC, contributing to the chain length and adding another layer of complexity at the systems level (Golks et al., 2006b). In addition, procaspase-8 dimerization and processing would further increase the number of differential equations. Therefore, an ODE approach was inappropriate to model this stoichiometry of the DISC.

After considering ODEs and other formalisms, we decided to make use of agent-based modeling (ABM) (see the Supplemental Information for more details) (Macal and North, 2009). In ABM, a system is modeled discretely in space and time as a collection of agents, which are autonomous decision-making entities. Here, one DISC was considered as a whole system and "an agent" corresponded to an individual molecule involved in DISC formation, i.e., CD95, FADD, procaspase-8, c-FLIP$_L$, and c-FLIP$_R$. Each agent/molecule could act based on a set of rules, which were based on its biological functions. These rules were the following. We did not have a limit to the number of agents at the DISC, i.e., the length of chains. In ABM we easily implemented generation of procaspase-8 chains and formation of homodimers and heterodimers with c-FLIP. In addition, procaspase-8 cleavage was considered to use intradimer and interdimer mechanisms (Chang et al., 2003), but only within one chain bound to the same receptor. The position for each individual agent, i.e., each individual procaspase-8 molecule within the chain, was defined. It has to be mentioned that all these rules could only be implemented in ABM, as in an ODE model this information would be lost.

A drawback of ABM is that reaction kinetics cannot be implied proportional to the molecule concentrations similar to the way they are used in ODE modeling. In our model, the recruitment of molecules to the DISC and processing of procaspase-8 were modeled by stochastic processes. Kinetics for the recruitment to the DISC were assumed as probabilities. The values of the recruitment probabilities were indirectly proportional to the distance of the respective molecule to the activated receptor.

To estimate the recruitment probabilities of molecules to the DISC, we needed to consider distances within a cell. Hence, a single cell was modeled as a three-dimensional grid (Figure 5A). The size of the grid was calculated from the ratio of the volume of a single cell compared to the total volume of all other DISC proteins, i.e., procaspase-8, FADD, c-FLIP$_L$, and c-FLIP$_R$ (Figure S3A, Supplemental Information). The receptors were placed in one plane representing the membrane. All other molecules were randomly distributed within the grid representing the cytosol (Figure 5A). Furthermore, on the basis of previous work, it was considered that c-FLIP has a higher affinity to the DISC compared to procaspase-8, which increases the recruitment probability relative to procaspase-8 (Bentele et al., 2004; Chang et al., 2002; Lavrik et al., 2007). Based on these assumptions, the values of the kinetic constants of recruitment probabilities were estimated (Table S5).

On the basis of the interaction rules between DISC proteins described above and estimated parameters, the mathematical model was generated (Figure 4B, Figure S3B, Supplemental Information). The model was calibrated using experimental data of procaspase-8 processing in SKW6.4 cells upon 1 μg/ml CD95L stimulation (Figures 5B and 5C, Figure S3C, Figure S4). The model efficiently simulated procaspase-8 (p55/p53) recruitment and processing (blue lines) for different CD95L stimulation strength (Figure 5C). However, a difference in the amount of p18 (red lines) in the cell was observed in simulations versus experimental data (Figure 5C). We assumed that these discrepancies were probably due to the much too high degradation rate of p18 in our current model based on previous work (Bentele et al., 2004). The model could also describe procaspase-8 processing in an independent cell line, i.e., HeLa cells, upon strong CD95 stimulation (Figure S5). Therefore, we concluded that our model is suitable to describe procaspase-8 processing in chains at the DISC upon strong CD95 stimulation.

Interestingly, the model failed to reproduce experimental data in SKW6.4 cells for 1 ng/ml CD95L stimulation (Figure 5C). According to the model, CD95 stimulation with 1 ng/ml CD95L results in procaspase-8 processing (blue line) and generation of active p18 (red line) (Figure 5C). This contradicts the previously reported mechanism of threshold behavior, which was observed in SKW6.4 cells upon CD95 stimulation with 1 ng/ml, and the experimental data, as procaspase-8 processing was already blocked upon even higher concentrations of 10 ng/ml CD95L (Figure 5C). The threshold mechanism implies inhibition of procaspase-8 activation upon low CD95 stimulation, as the low number of active receptors will be blocked by c-FLIP proteins due to their higher affinity to the DISC (Bentele et al., 2004; Lavrik et al., 2007). From these observations, we concluded that we are missing some essential assumptions for modeling the chain formation and, thus, focused our attention on the composition of the DED chains and their length.

Figure 4. Topology of the Model

(A) Biochemical scheme of the DISC model. Upon stimulation of CD95, FADD is recruited first to form an active DISC. Subsequently, procaspase-8, c-FLIP$_L$, and c-FLIP$_R$ are recruited and form chains via DED interactions. Procaspase-8 homodimers can be processed to p10$_2$–p18$_2$ via the intermediate p43/p41.

(B) Topology of the CD95 DISC model. DED chains are shown in gray. Dimers of DED proteins are highlighted in green. Red arrows indicate catalytic processing of procaspase-8. The schematic topology shows the combinatorial complexity of the model.

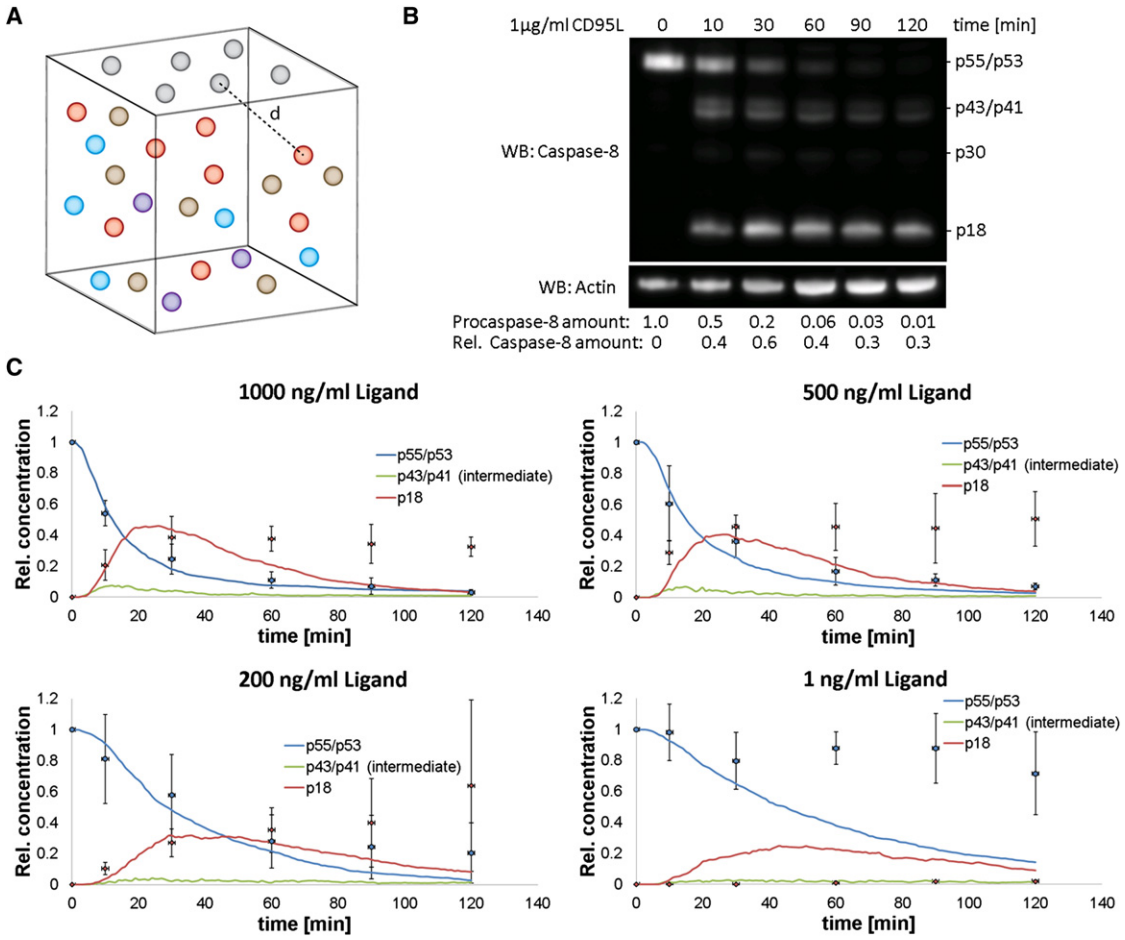

Figure 5. Model Calibration

(A) We modeled our system in a single cell represented as a three-dimensional grid. CD95 receptors (gray) were placed in one plane, representing the plasma membrane, while all other molecules, i.e., procaspase-8, FADD, c-FLIP$_L$, and c-FLIP$_R$, were randomly placed within the grid, representing the cytosol.

(B) Representative western blot of procaspase-8 processing in SKW6.4 cells used for model calibration. All western blots used for model calibration can be found in Figure S4.

(C) Time courses of procaspase-8 processing in SKW6.4 cells for different strengths of CD95 stimulation. Simulations are shown as solid lines, and experimental data are shown as individual dots including standard deviation. The simulation of procaspase-8 processing for 1 ng/ml CD95L is shown in one diagram with experimental data obtained for 10 ng/ml CD95L and indicates that procaspase-8 processing is already significantly inhibited upon higher CD95 stimulation strength. Procaspase-8 processing in SKW6.4 cells was repeated seven times for 1 µg/ml CD95L and three times for the other CD95L concentrations.

Modeling and Mass Spectrometry Analysis Revealed the Optimal Stoichiometry for Procaspase-8 Activation at the DISC

As pointed out above, the initial model could not describe procaspase-8 processing upon low CD95 stimulation strength. In the initial model, we assumed that procaspase-8 chains are formed without any restriction (Figure 5). However, there has to be a mechanism of chain length restriction in the cell; otherwise, apoptosis could be induced upon activation of only few receptors. Furthermore, as the amount of procaspase-8 in the cell is limited, it is likely that there is a natural restriction of chain length. Therefore, we added another parameter to the model, which described the chain restriction and was introduced as a maximally allowed chain length per receptor. Consequently, DED proteins could only form chains in silico up to a defined maximal length.

Next, we used the model with chain length restriction to study how different chain lengths, resulting in different stoichiometric ratios between procaspase-8 and FADD, translate into efficient caspase-8 activation. We computed a two-dimensional phase diagram of caspase-8 activation at the DISC depending on the chain length (Figure 6A). Simulations predicted that chains from two to four procaspase-8 molecules would result in active caspase-8 for CD95 stimulations with 200, 500, and 1,000 ng/ml CD95L (Figure 6A, Figure S6). Modeling on the basis of experimental data of caspase-8 activation in HeLa cells also suggested that efficient processing of procaspase-8 requires chains longer than two molecules (Figure S7). Remarkably, as can be seen from the diagram, the threshold behavior, i.e., inhibition of caspase-8 activation upon CD95 stimulation with 1 ng/ml, could occur only upon chain lengths lower than eight (Figure 6A, Figure S8). Therefore, we propose that the optimal

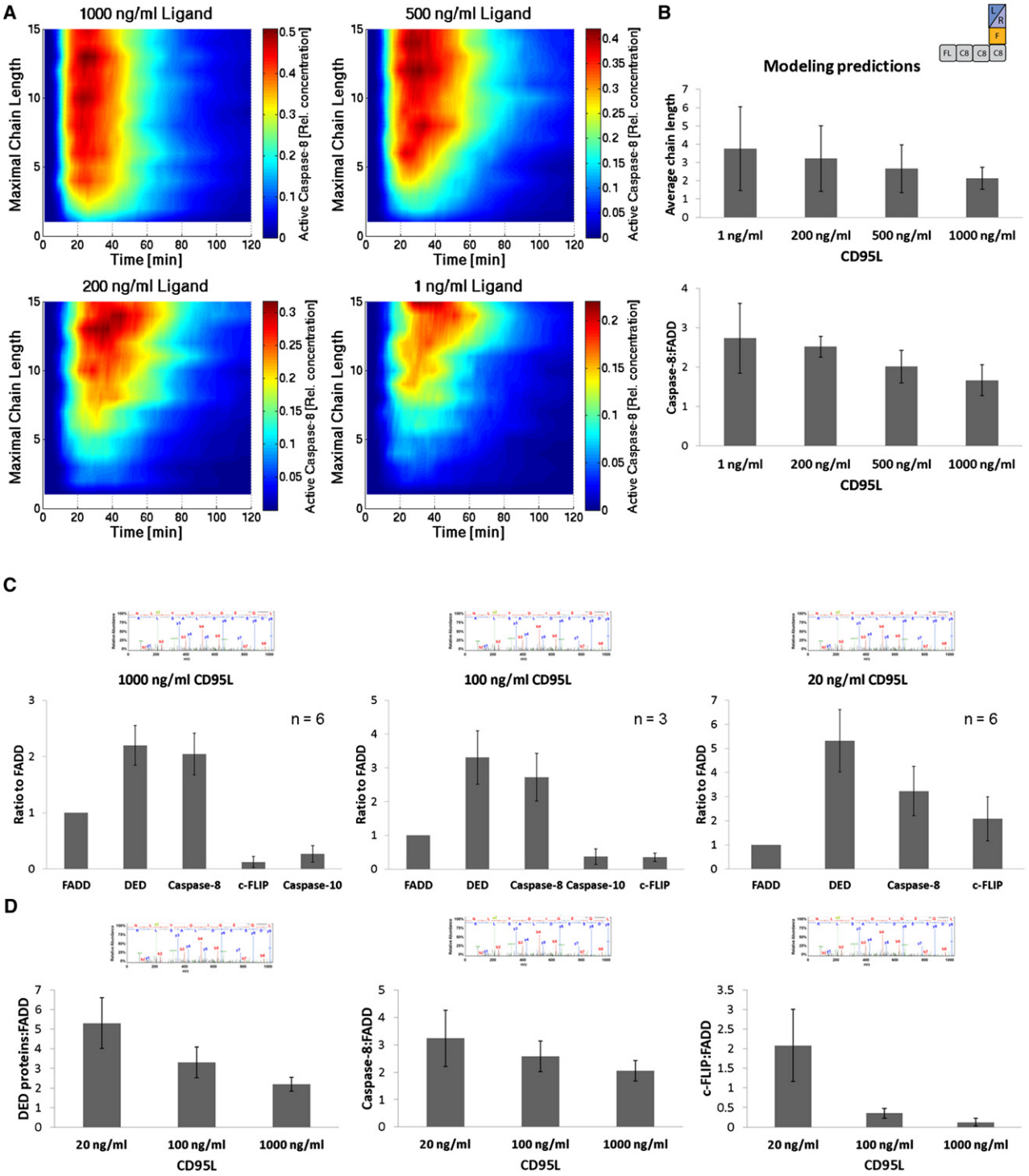

Figure 6. The Model Predicts Stimulus-Strength-Dependent Chain Lengths and Is Verified by Mass Spectrometry

(A) Two-dimensional diagram demonstrating simulations of the amount of the active caspase-8 depending upon CD95 stimulation strength and the maximum chain length allowed.

(B) Simulations of the length of procaspase-8 chains and the ratio of procaspase-8/FADD depending upon CD95 stimulation strength. The model predicts that upon weaker CD95 stimulation the average chain length increases.

(C and D) Ratios of DED proteins to FADD in SKW6.4 cells for CD95 stimulation with 20, 100, and 1,000 ng/ml CD95L obtained by Orbitrap-MS. Upon low CD95 stimulation, MS analysis indicates enrichment of c-FLIP at the DISC and an increase of a chain length as predicted by the model. The mean ± SD of multiple experiments is shown.

Please cite this article in press as: Schleich et al., Stoichiometry of the CD95 Death-Inducing Signaling Complex: Experimental and Modeling Evidence for a Death Effector Domain Chain Model, Molecular Cell (2012), doi:10.1016/j.molcel.2012.05.006

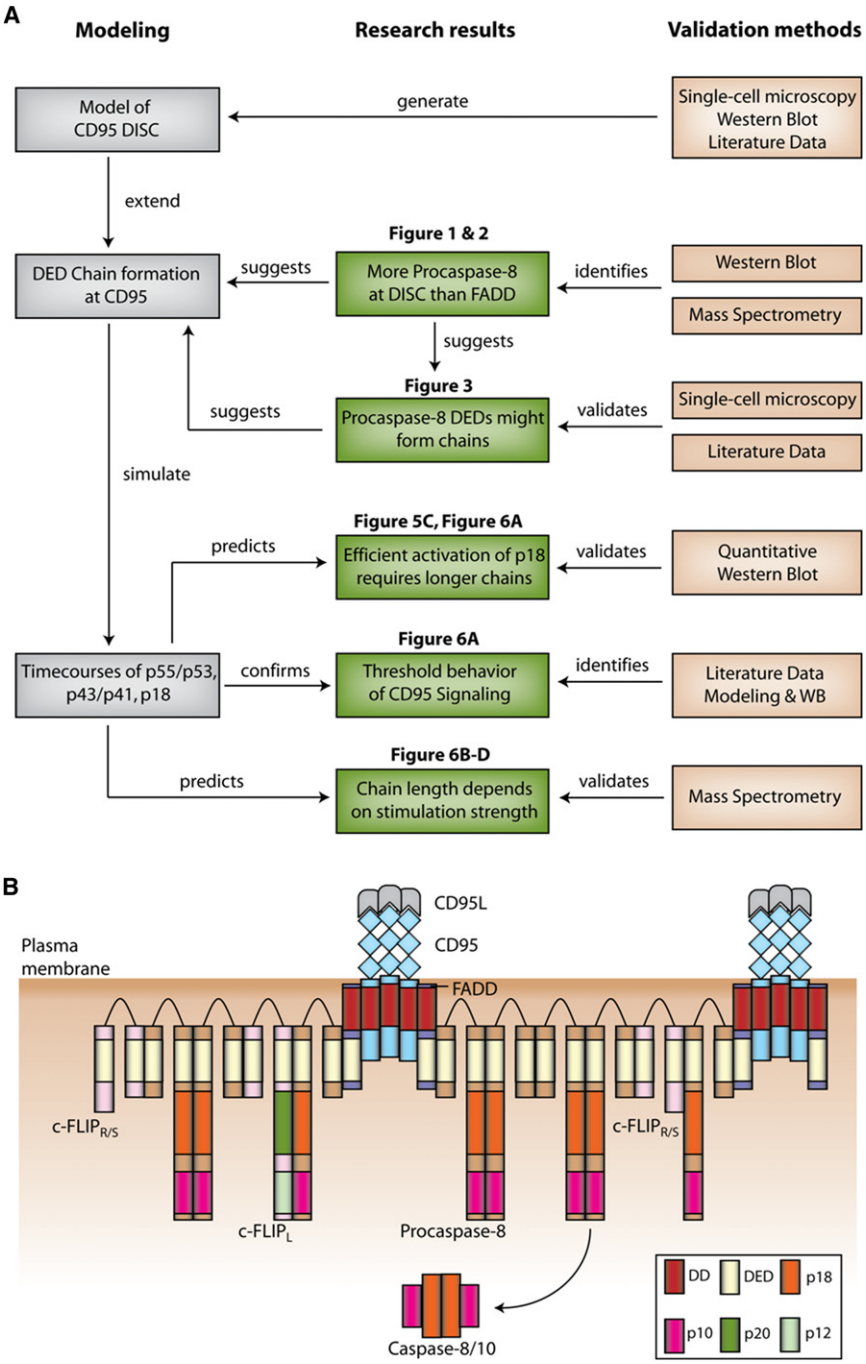

Figure 7. The Model of the CD95 DISC

(A) Workflow of experimental findings, model predictions, and experimental validations.

(B) Model of the CD95 DISC. Procaspase-8/procaspase-10 and c-FLIP form a platform at the DISC, which enables dimerization of procaspase-8 and efficient activation. The length of chains may be restricted by the formation of bridges between neighboring receptors.

procaspase-8 chain length for procaspase-8 activation is between two to eight molecules of DED proteins per receptor.

The shape of the two-dimensional diagram implied that procaspase-8 chain length at the DISC is determined by CD95 stimulation strength (Figure 6A). We further analyzed how CD95 stimulation strength influences procaspase-8 chain length. Interestingly, the model predicted that the average DED chain is shorter upon stronger CD95 stimulation (Figure 6B, Figure S8).

We tested these model predictions experimentally by performing MS analysis of the DISC (Figures 6C and 6D, Table S6, and Table S7). We stimulated SKW6.4 cells with lower concentrations of CD95L and performed MS analysis similar to that described above in Figure 2. We had to use more cells for the analysis, as the amount of immunoprecipitated DISCs significantly decreased upon lower stimulation. We could show that upon low CD95 stimulation strength the DED:FADD ratio increased compared to high CD95 stimulation strength, indicating longer chains (Figure 6D). Furthermore, c-FLIP amounts at the DISC were increased upon lower CD95 stimulation (Figure 6D). This is in accordance with previous reports on the mechanism of the inhibitory role of c-FLIP upon low CD95 stimulation strength that is based on the higher affinity of c-FLIP to the DISC compared to procaspase-8 (Bentele et al., 2004; Lavrik et al., 2007). Thus, we concluded that the length of the chains is strongly dependent on CD95 stimulation strength.

To explore further mechanisms of DED chain dynamics, we investigated the influence of procaspase-8 turnover at the DISC on the chain length. Simulations show that less-stable binding of procaspase-8 and higher turnover rates led to activation with shorter chains of procaspase-8 (Figure S9). On the basis of these simulations, we concluded that turnover rates of procaspase-8 can directly influence procaspase-8 chain length and, therefore, caspase-8 activation.

Taken together, the mathematical model well described the stoichiometry of the DISC with procaspase-8 chains. The biological information based on our own experiments and the literature search has been translated into the model as it is shown in Figure 7A. The model was supported and validated by western blot and MS (Figure 7A). Furthermore, this approach did not only allow us to mechanistically describe procaspase-8 activation

in DED chains, but also to quantitatively define how the dynamics of the DED protein chain length influences procaspase-8 activation and, thereby, DR-induced apoptosis.

DISCUSSION

Our findings provide evidence that procaspase-8/procaspase-10 and c-FLIP form DED platforms at the DISC. These platforms might be formed with chains of each of these DED proteins attached to one FADD (Figure 7B). In this way, procaspase-8 can form homodimers and heterodimers with c-FLIP$_L$ leading to caspase activation. This is a more direct explanation of how procaspase-8 homodimers and heterodimers can be formed at the DISC, which is an essential step for initiator caspase activation (Fuentes-Prior and Salvesen, 2004; Krammer et al., 2007; Lavrik et al., 2005; Oberst et al., 2010). In addition, our findings also support the interdimer model of procaspase-8 activation, suggesting activation of one procaspase-8 dimer by a neighboring procaspase-8 dimer in the chain (Chang et al., 2003).

Different methods provided various estimations of the length of the DED chains at the DISC. Quantitative MS experiments with several sets of AQUA peptides and two different mass spectrometers, QTRAP and Orbitrap, have shown that there are two to three DED proteins per FADD at the DISC. Quantitative western blot demonstrated five DED proteins per FADD. Quantitative western blot and MS values are not exactly comparable, but overall the results point to a higher amount of procaspase-8 compared to FADD in the DISC. Interestingly, in the study by Dickens et al. (2012; in this issue of *Molecular Cell*), the authors obtained even longer procaspase-8 chains than we did. Dickens et al. isolated the DISCs via sucrose gradients and collected only the high molecular weight fraction with high molecular weight DISC aggregates. In our study, we immunoprecipitated all activated CD95, which naturally results in the pull-down of DISCs with longer chains and "smaller" DISCs, which might even have only FADD bound. Therefore, we measured procaspase-8 chains at the DISC averaged over the DISCs with long and short chains. This might have led to the fact that we came up with shorter procaspase-8 chains than did Dickens et al. Furthermore, Dickens et al. analyzed the TRAIL DISC composition, while we concentrated on the CD95 DISC, which might have led to the differences.

Although we applied quantitative experimental methods in our study, we only obtained an average stoichiometry of the DISC, and we needed mathematical modeling to gain more insight into dynamics of the procaspase-8 chains (Figure 7A). We found that the length of procaspase-8 chains is variable and depends on several factors, such as CD95 stimulation strength, concentration of procaspase-8 in the cell, and affinity of procaspase-8 to the DISC. The stimulation strength is one of the most important factors defining the length of the chains. We have shown experimentally and in silico that low CD95 stimulation results in longer chains. Longer chains should create more sites for procaspase-8 activation and compensate for the low number of activated receptors. Dynamic control of the length of procaspase-8 chains could play an important role in the regulation of procaspase-8 activation.

Another important outcome of our study is the restriction of the procaspase-8 chain length at the DISC. This can result from the fact that the average chain length is defined by the strength of stimulation and by the ratio between the number of stimulated receptors and cellular levels of procaspase-8. Given that there is a limited number of procaspase-8 in the cell, which slightly exceeds the number of receptors, the probability of procaspase-8 chains longer than ten is very low. The model found a restriction of the length of the chains up to eight. This is also obvious from the biological point of view, as a nonlimited size of DED chains would imply induction of apoptosis upon stimulation of only a few receptors. As the cell should develop protection mechanisms from spontaneous apoptosis, this scenario should obviously be excluded. Possible mechanisms of chain restriction could include the interaction of DISC-bound procaspase-8 attached to different receptors to form DED bridges between neighboring receptors, limited concentration of procaspase-8 in the cell, and turnover of procaspase-8 at the DISC.

Recently, a number of X-ray structures of CD95 interacting with FADD have been obtained (Scott et al., 2009; Wang et al., 2010). Wang et al. proposed the core DISC structure to be composed of five to seven CD95 DD and five FADD DD, while Scott et al. proposed that the core DISC structure has a tetrameric configuration of four CD95 DD and four FADD DD. In our work we considered interactions of caspase-8 with FADD and did not focus on the events upstream of FADD.

Several insights into CD95 signaling are supported by our model. Chains of procaspase-8 at the DISC should also provide ideal platforms for polyubiquitination and aggregation of procaspase-8 at the DISC, as recently reported (Jin et al., 2009). We and others have shown the generation of complex II upon CD95 stimulation (Geserick et al., 2009; Lavrik et al., 2008). Complex II comprises DED-proteins, i.e., procaspase-8, FADD, and c-FLIP, but does not contain CD95. The mechanism of complex II formation remains unclear, but it might be connected to the aggregation of caspase-8 and c-FLIP in DED platforms. It is likely that when DED platforms reach a certain size, they might dissociate into the cytosol. The presence of DED platforms in the cytosol might facilitate apoptosis by cleavage of cytosolic substrates of caspase-8 such as Bid and caspase-3/caspase-7.

Another interesting aspect of our model is that it may explain how different forms of ligand influence the DISC stoichiometry. It was convincingly shown by O'Reilly and coworkers that the membrane-bound CD95 ligand, but not the soluble one, is critical for apoptosis (O'Reilly et al., 2009). An independent line of evidence indicates that the binding of the ligand leads to a conformational change in the DD of CD95, allowing FADD recruitment (Scott et al., 2009). We assume that the binding of the membrane-bound ligand results in a more stable receptor/ligand complex compared to the one formed by a soluble ligand, possibly via stabilization of the conformational change of the CD95 DD and facilitation of FADD recruitment. This complex may provide a more stable platform for the elongation of procaspase-8 chains.

There are several mutations in the DED proteins, which support our model of the DISC. The FADD-DN mutants,

described to have a severe effect on apoptosis, should prevent formation of a functional DED chain (Newton et al., 1998). Furthermore, caspase-8 is mutated in numerous carcinomas (Kim et al., 2003; Soung et al., 2005a, 2005b). These mutations also reside within the DEDs of procaspase-8. Even though these mutants still interact with FADD, they might interfere with chain formation, thus interfering with procaspase-8 activation. Furthermore, caspase-8 mutations can lead to defective activation of lymphocytes and immunodeficiency (Chun et al., 2002).

Taken together, our data provide an unexpected view on CD95 DISC organization as well as procaspase-8 activation at the DISC and initiation of apoptosis. The powerful methodology might be applied to the analysis of other cell death-inducing complexes such as the ripoptosome or necrosome and for complexes derived from diseases with defects in cell death pathways (Feoktistova et al., 2011; Haas et al., 2009; Tenev et al., 2011).

EXPERIMENTAL PROCEDURES

Cell Lines

SKW6.4 cells were maintained in RPMI (Life Technologies, Germany), 10 mM HEPES (Life Technologies, Germany), 50 μg/ml gentamycin (Life Technologies, Germany), and 10% fetal calf serum (Life Technologies, Germany) in 5% CO_2. HeLa-CD95 cells (Neumann et al., 2010) were generated by selection with 20 ng/ml puromycin according to standard protocols and maintained in DMEM (Life Technologies, Germany), 10 mM HEPES (Life Technologies, Germany), 50 μg/ml gentamycin (Life Technologies, Germany), and 10% fetal calf serum (Life Technologies, Germany) in 5% CO_2. Transfections were done using Lipofectamine 2000 (Invitrogen, Germany).

Antibodies and Reagents

Anti-caspase-8 monoclonal antibody C15 (mouse IgG2b) recognizes the p18 subunit of caspase-8 (Scaffidi et al., 1997). Anti-FLIP monoclonal antibody NF6 (mouse IgG1) recognizes the N-terminal part of c-FLIP (Scaffidi et al., 1999). Anti-FADD monoclonal antibody 1C4 (mouse IgG1) recognizes the C-terminal part of FADD (Scaffidi et al., 2000). Anti-APO-1 (anti-CD95) is an agonistic monoclonal antibody (IgG3) recognizing an epitope at the extracellular part of CD95 (Trauth et al., 1989). Horseradish peroxidase-conjugated goat anti-mouse IgG1, IgG2a, and IgG2b were obtained from Southern Biotech. The coding sequence of LZ-CD95L (Walczak et al., 1999) was cloned into a pIRESpuro3 plasmid (Takara Bio Inc.). Recombinant LZ-CD95L was produced using 293T cells stably transfected with this vector. All chemicals used were of analytical grade and purchased from Merck or Sigma-Aldrich.

A full description of experimental procedures can be found in the Supplemental Information.

SUPPLEMENTAL INFORMATION

Supplemental Information includes nine figures and seven tables can be found with this article online at doi:10.1016/j.molcel.2012.05.006.

ACKNOWLEDGMENTS

This work was supported by the Initiative and Networking Fund of the Helmholtz Association within the Helmholtz Alliance on Systems Biology/SBCancer and Helmholtz-Russia Joint Research Groups-2008-2. We thank Ramona Mayer, Vera Seiler, and Jennifer Hölzel for technical assistance; Joel Beaudouin for discussions and advice with microscopy; Roland Eils for discussions; Thomas Ruppert and Sebastian Link from the DKFZ-ZMBH Alliance for QTRAP assistance; and Justin Feigelman, Claudia Weber, and Karsten Gülow for critical reading of this manuscript.

Received: November 7, 2011
Revised: March 27, 2012
Accepted: May 3, 2012
Published online: June 7, 2012

REFERENCES

Aebersold, R., and Mann, M. (2003). Mass spectrometry-based proteomics. Nature *422*, 198–207.

Albeck, J.G., Burke, J.M., Aldridge, B.B., Zhang, M., Lauffenburger, D.A., and Sorger, P.K. (2008). Quantitative analysis of pathways controlling extrinsic apoptosis in single cells. Mol. Cell *30*, 11–25.

Aldridge, B.B., Gaudet, S., Lauffenburger, D.A., and Sorger, P.K. (2011). Lyapunov exponents and phase diagrams reveal multi-factorial control over TRAIL-induced apoptosis. Mol. Syst. Biol. *7*, 1–21.

Bentele, M., Lavrik, I., Ulrich, M., Stösser, S., Heermann, D.W., Kalthoff, H., Krammer, P.H., and Eils, R. (2004). Mathematical modeling reveals threshold mechanism in CD95-induced apoptosis. J. Cell Biol. *166*, 839–851.

Carrington, P.E., Sandu, C., Wei, Y., Hill, J.M., Morisawa, G., Huang, T., Gavathiotis, E., Wei, Y., and Werner, M.H. (2006). The structure of FADD and its mode of interaction with procaspase-8. Mol. Cell *22*, 599–610.

Chang, D.W., Xing, Z., Pan, Y., Algeciras-Schimnich, A., Barnhart, B.C., Yaish-Ohad, S., Peter, M.E., and Yang, X. (2002). c-FLIP(L) is a dual function regulator for caspase-8 activation and CD95-mediated apoptosis. EMBO J. *21*, 3704–3714.

Chang, D.W., Xing, Z., Capacio, V.L., Peter, M.E., and Yang, X. (2003). Interdimer processing mechanism of procaspase-8 activation. EMBO J. *22*, 4132–4142.

Chen, C., Cui, J., Lu, H., Wang, R., Zhang, S., and Shen, P. (2007). Modeling of the role of a Bax-activation switch in the mitochondrial apoptosis decision. Biophys. J. *92*, 4304–4315.

Chun, H.J., Zheng, L., Ahmad, M., Wang, J., Speirs, C.K., Siegel, R.M., Dale, J.K., Puck, J., Davis, J., Hall, C.G., et al. (2002). Pleiotropic defects in lymphocyte activation caused by caspase-8 mutations lead to human immunodeficiency. Nature *419*, 395–399.

Dickens, L.S., Boyd, R.S., Jukes-Jones, R., Hughes, M.A., Robinson, G.L., Fairall, L., Schwabe, J.W.R., Cain, K., and MacFarlane, M. (2012). A death effector domain chain DISC model reveals a crucial role for caspase-8 chain assembly in mediating apoptotic cell death. Mol. Cell *47*, this issue, ■■■–■■■.

Feoktistova, M., Geserick, P., Kellert, B., Dimitrova, D.P., Langlais, C., Hupe, M., Cain, K., MacFarlane, M., Häcker, G., and Leverkus, M. (2011). cIAPs block Ripoptosome formation, a RIP1/caspase-8 containing intracellular cell death complex differentially regulated by cFLIP isoforms. Mol. Cell *43*, 449–463.

Fricker, N., Beaudouin, J., Richter, P., Eils, R., Krammer, P.H., and Lavrik, I.N. (2010). Model-based dissection of CD95 signaling dynamics reveals both a pro- and antiapoptotic role of c-FLIPL. J. Cell Biol. *190*, 377–389.

Fuentes-Prior, P., and Salvesen, G.S. (2004). The protein structures that shape caspase activity, specificity, activation and inhibition. Biochem. J. *384*, 201–232.

Fussenegger, M., Bailey, J.E., and Varner, J. (2000). A mathematical model of caspase function in apoptosis. Nat. Biotechnol. *18*, 768–774.

Gerber, S.A., Rush, J., Stemman, O., Kirschner, M.W., and Gygi, S.P. (2003). Absolute quantification of proteins and phosphoproteins from cell lysates by tandem MS. Proc. Natl. Acad. Sci. USA *100*, 6940–6945.

Geserick, P., Hupe, M., Moulin, M., Wong, W.W.-L., Feoktistova, M., Kellert, B., Gollnick, H., Silke, J., and Leverkus, M. (2009). Cellular IAPs inhibit a cryptic CD95-induced cell death by limiting RIP1 kinase recruitment. J. Cell Biol. *187*, 1037–1054.

Golks, A., Brenner, D., Fritsch, C., Krammer, P.H., and Lavrik, I.N. (2005). c-FLIPR, a new regulator of death receptor-induced apoptosis. J. Biol. Chem. *280*, 14507–14513.

Golks, A., Brenner, D., Krammer, P.H., and Lavrik, I.N. (2006a). The c-FLIP-NH2 terminus (p22-FLIP) induces NF-kappaB activation. J. Exp. Med. *203*, 1295–1305.

Golks, A., Brenner, D., Schmitz, I., Watzl, C., Krueger, A., Krammer, P.H., and Lavrik, I.N. (2006b). The role of CAP3 in CD95 signaling: new insights into the mechanism of procaspase-8 activation. Cell Death Differ. *13*, 489–498.

Haas, T.L., Emmerich, C.H., Gerlach, B., Schmukle, A.C., Cordier, S.M., Rieser, E., Feltham, R., Vince, J., Warnken, U., Wenger, T., et al. (2009). Recruitment of the linear ubiquitin chain assembly complex stabilizes the TNF-R1 signaling complex and is required for TNF-mediated gene induction. Mol. Cell *36*, 831–844.

Heiner, M., Koch, I., and Will, J. (2004). Model validation of biological pathways using Petri nets—demonstrated for apoptosis. Biosystems *75*, 15–28.

Hoffmann, J.C., Pappa, A., Krammer, P.H., and Lavrik, I.N. (2009). A new C-terminal cleavage product of procaspase-8, p30, defines an alternative pathway of procaspase-8 activation. Mol. Cell. Biol. *29*, 4431–4440.

Hughes, M.A., Harper, N., Butterworth, M., Cain, K., Cohen, G.M., and MacFarlane, M. (2009). Reconstitution of the death-inducing signaling complex reveals a substrate switch that determines CD95-mediated death or survival. Mol. Cell *35*, 265–279.

Jin, Z., Li, Y., Pitti, R., Lawrence, D., Pham, V.C., Lill, J.R., and Ashkenazi, A. (2009). Cullin3-based polyubiquitination and p62-dependent aggregation of caspase-8 mediate extrinsic apoptosis signaling. Cell *137*, 721–735.

Kim, H.S., Lee, J.W., Soung, Y.H., Park, W.S., Kim, S.Y., Lee, J.H., Park, J.Y., Cho, Y.G., Kim, C.J., Jeong, S.W., et al. (2003). Inactivating mutations of caspase-8 gene in colorectal carcinomas. Gastroenterology *125*, 708–715.

Krammer, P.H. (2000). CD95's deadly mission in the immune system. Nature *407*, 789–795.

Krammer, P.H., Arnold, R., and Lavrik, I.N. (2007). Life and death in peripheral T cells. Nat. Rev. Immunol. *7*, 532–542.

Lange, V., Picotti, P., Domon, B., and Aebersold, R. (2008). Selected reaction monitoring for quantitative proteomics: a tutorial. Mol. Syst. Biol. *4*, 222. 10.1038/msb.2008.61.

Langenfeld, E., Zanger, U.M., Jung, K., Meyer, H.E., and Marcus, K. (2009). Mass spectrometry-based absolute quantification of microsomal cytochrome P450 2D6 in human liver. Proteomics *9*, 2313–2323.

Lavrik, I.N. (2010). Systems biology of apoptosis signaling networks. Curr. Opin. Biotechnol. *95*, 3–7.

Lavrik, I.N., Golks, A., and Krammer, P.H. (2005). Caspases: pharmacological manipulation of cell death. J. Clin. Invest. *115*, 2665–2672.

Lavrik, I.N., Golks, A., Riess, D., Bentele, M., Eils, R., and Krammer, P.H. (2007). Analysis of CD95 threshold signaling: triggering of CD95 (FAS/APO-1) at low concentrations primarily results in survival signaling. J. Biol. Chem. *282*, 13664–13671.

Lavrik, I.N., Mock, T., Golks, A., Hoffmann, J.C., Baumann, S., and Krammer, P.H. (2008). CD95 stimulation results in the formation of a novel death effector domain protein-containing complex. J. Biol. Chem. *283*, 26401–26408.

Li, F.-Y., Jeffrey, P.D., Yu, J.W., and Shi, Y. (2006). Crystal structure of a viral FLIP: insights into FLIP-mediated inhibition of death receptor signaling. J. Biol. Chem. *281*, 2960–2968.

Macal, C.M., and North, M.J. (2009). Agent-based modeling and simulation. Proceedings of the 2009 Winter Simulation Conference (WSC), 86–98.

Muzio, M., Chinnaiyan, A.M., Kischkel, F.C., O'Rourke, K., Shevchenko, A., Ni, J., Scaffidi, C., Bretz, J.D., Zhang, M., Gentz, R., et al. (1996). FLICE, a novel FADD-homologous ICE/CED-3-like protease, is recruited to the CD95 (Fas/APO-1) death–inducing signaling complex. Cell *85*, 817–827.

Neumann, L., Pforr, C., Beaudouin, J., Pappa, A., Fricker, N., Krammer, P.H., Lavrik, I.N., and Eils, R. (2010). Dynamics within the CD95 death-inducing signaling complex decide life and death of cells. Mol. Syst. Biol. *6*, 352. 10.1038/msb.2010.6.

Newton, K., Harris, W., Bath, M.L., Smith, K.G., and Strasser, A. (1998). A dominant interfering mutant of FADD/MORT1 enhances deletion of autoreactive thymocytes and inhibits proliferation of mature T lymphocytes. EMBO J. *17*, 706–718.

Oberst, A., Pop, C., Tremblay, A.G., Blais, V., Denault, J.-B., Salvesen, G.S., and Green, D.R. (2010). Inducible dimerization and inducible cleavage reveal a requirement for both processes in caspase-8 activation. J. Biol. Chem. *285*, 16632–16642.

Olsen, J.V., de Godoy, L.M.F., Li, G., Macek, B., Mortensen, P., Pesch, R., Makarov, A., Lange, O., Horning, S., and Mann, M. (2005). Parts per million mass accuracy on an Orbitrap mass spectrometer via lock mass injection into a C-trap. Mol. Cell Proteomics *4*, 2010–2021.

O'Reilly, L.A., Tai, L., Lee, L., Kruse, E.A., Grabow, S., Fairlie, W.D., Haynes, N.M., Tarlinton, D.M., Zhang, J.-G., Belz, G.T., et al. (2009). Membrane-bound Fas ligand only is essential for Fas-induced apoptosis. Nature *461*, 659–663.

Peter, M.E., and Krammer, P.H. (2003). The CD95(APO-1/Fas) DISC and beyond. Cell Death Differ. *10*, 26–35.

Peter, M.E., Budd, R.C., Desbarats, J., Hedrick, S.M., Hueber, A.-O., Newell, M.K., Owen, L.B., Pope, R.M., Tschopp, J., Wajant, H., et al. (2007). The CD95 receptor: apoptosis revisited. Cell *129*, 447–450.

Rehm, M., Huber, H.J., Dussmann, H., and Prehn, J.H.M. (2006). Systems analysis of effector caspase activation and its control by X-linked inhibitor of apoptosis protein. EMBO J. *25*, 4338–4349.

Scaffidi, C., Medema, J.P., Krammer, P.H., and Peter, M.E. (1997). FLICE is predominantly expressed as two functionally active isoforms, caspase-8/a and caspase-8/b. J. Biol. Chem. *272*, 26953–26958.

Scaffidi, C., Fulda, S., Srinivasan, A., Friesen, C., Li, F., Tomaselli, K.J., Debatin, K.M., Krammer, P.H., and Peter, M.E. (1998). Two CD95 (APO-1/Fas) signaling pathways. EMBO J. *17*, 1675–1687.

Scaffidi, C., Schmitz, I., Krammer, P.H., and Peter, M.E. (1999). The role of c-FLIP in modulation of CD95-induced apoptosis. J. Biol. Chem. *274*, 1541–1548.

Scaffidi, C., Volkland, J., Blomberg, I., Hoffmann, I., Krammer, P.H., and Peter, M.E. (2000). Phosphorylation of FADD/ MORT1 at serine 194 and association with a 70-kDa cell cycle-regulated protein kinase. J. Immunol. *164*, 1236–1242.

Schlatter, R., Schmich, K., Avalos Vizcarra, I., Scheurich, P., Sauter, T., Borner, C., Ederer, M., Merfort, I., and Sawodny, O. (2009). ON/OFF and beyond—a boolean model of apoptosis. PLoS Comput. Biol. *5*, e1000595. 10.1371/journal.pcbi.1000595.

Scott, F.L., Stec, B., Pop, C., Dobaczewska, M.K., Lee, J.J., Monosov, E., Robinson, H., Salvesen, G.S., Schwarzenbacher, R., and Riedl, S.J. (2009). The Fas-FADD death domain complex structure unravels signalling by receptor clustering. Nature *457*, 1019–1022.

Siegel, R.M., Martin, D.a., Zheng, L., Ng, S.Y., Bertin, J., Cohen, J., and Lenardo, M.J. (1998). Death-effector filaments: novel cytoplasmic structures that recruit caspases and trigger apoptosis. J. Cell Biol. *141*, 1243–1253.

Soung, Y.H., Lee, J.W., Kim, S.Y., Jang, J., Park, Y.G., Park, W.S., Nam, S.W., Lee, J.Y., Yoo, N.J., and Lee, S.H. (2005a). CASPASE-8 gene is inactivated by somatic mutations in gastric carcinomas. Cancer Res. *65*, 815–821.

Soung, Y.H., Lee, J.W., Kim, S.Y., Sung, Y.J., Park, W.S., Nam, S.W., Kim, S.H., Lee, J.Y., Yoo, N.J., and Lee, S.H. (2005b). Caspase-8 gene is frequently inactivated by the frameshift somatic mutation 1225_1226delTG in hepatocellular carcinomas. Oncogene *24*, 141–147.

Sprick, M.R., Rieser, E., Stahl, H., Grosse-Wilde, A., Weigand, M.A., and Walczak, H. (2002). Caspase-10 is recruited to and activated at the native TRAIL and CD95 death-inducing signalling complexes in a FADD-dependent manner but can not functionally substitute caspase-8. EMBO J. *21*, 4520–4530.

Strasser, A., Jost, P.J., and Nagata, S. (2009). The many roles of FAS receptor signaling in the immune system. Immunity *30*, 180–192.

Tenev, T., Bianchi, K., Darding, M., Broemer, M., Langlais, C., Wallberg, F., Zachariou, A., Lopez, J., MacFarlane, M., Cain, K., and Meier, P. (2011). The Ripoptosome, a signaling platform that assembles in response to genotoxic stress and loss of IAPs. Mol. Cell *43*, 432–448.

Trauth, B.C., Klas, C., Peters, A.M., Matzku, S., Möller, P., Falk, W., Debatin, K.M., and Krammer, P.H. (1989). Monoclonal antibody-mediated tumor regression by induction of apoptosis. Science *245*, 301–305.

Walczak, H., Miller, R.E., Ariail, K., Gliniak, B., Griffith, T.S., Kubin, M., Chin, W., Jones, J., Woodward, A., Le, T., et al. (1999). Tumoricidal activity of tumor necrosis factor-related apoptosis-inducing ligand in vivo. Nat. Med. *5*, 157–163.

Wang, L., Yang, J.K., Kabaleeswaran, V., Rice, A.J., Cruz, A.C., Park, A.Y., Yin, Q., Damko, E., Jang, S.B., Raunser, S., et al. (2010). The Fas-FADD death domain complex structure reveals the basis of DISC assembly and disease mutations. Nat. Struct. Mol. Biol. *17*, 1324–1329.

Yang, J.K., Wang, L., Zheng, L., Wan, F., Ahmed, M., Lenardo, M.J., and Wu, H. (2005). Crystal structure of MC159 reveals molecular mechanism of DISC assembly and FLIP inhibition. Mol. Cell *20*, 939–949.